

BME 695N

Engineering Nanomedical Systems

Lecture 18

Designing nanodelivery systems for in-vivo use

James F. Leary, Ph.D.

SVM Endowed Professor of Nanomedicine
Professor of Basic Medical Sciences and
Biomedical Engineering

Member: Purdue Cancer Center; Oncological Sciences Center;
Bindley Biosciences Center; Birck Nanotechnology Center

Email: jfleary@purdue.edu

I. Overview – the *in-vitro* to *ex-vivo* to *in-vivo* paradigm

- A. In-vitro - importance of choosing suitable cell lines
- B. Ex-vivo – adding the complexity of in-vivo background while keeping the simplicity of in-vitro
- C. In-vivo - all the complexity of ex-vivo plus the “active” components of a real animal

II. In-vivo systems are open, “active” systems with multiple layers of complexity

- A. in-vitro and ex-vivo are mostly “closed” systems, but not absolutely
- B. what is an “open” system?
- C. attempts to isolate open systems

III. Layers of complexity of in-vivo systems

- A. human cells in nude mice – a mixture of in-vitro and in-vivo
- B. “model” small animal systems
- C. better-model, larger animal systems

IV. Examples of the in-vitro to in-vivo experimental pathway

A. Kopelman group – multifunctional NPs for MRI and photodynamic therapy

Source: Kopelman, R., Koo, Y-E, Philbert, M., Moffatc, B.A., Reddy, G.R., McConville, P., Hall, D.E., Chenevert, T.L., Bhojanie, M.S., Buck, S.M., Rehemtulla, A., Ross, B.D. Multifunctional nanoparticle platforms for in vivo MRI enhancement and photodynamic therapy of a rat brain cancer. *Journal of Magnetism and Magnetic Materials* 293: 404–410, 2005.

Development of a multifunctional nanomedical system

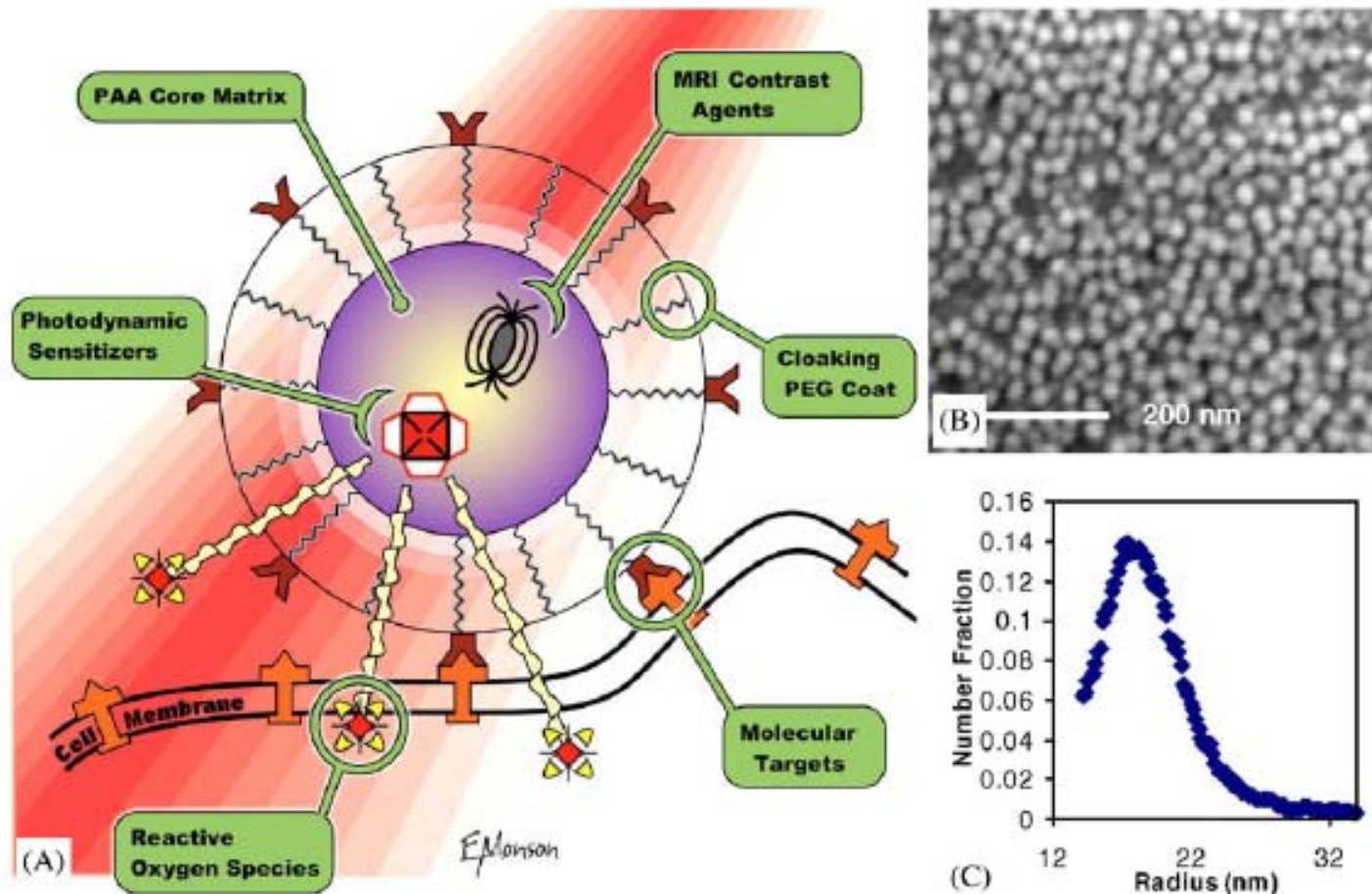


Fig. 1. Overview of nanoparticle platform. (A) Schematic nanoparticle platform with photodynamic dye, MRI contrast enhancement agent, polyethylene glycol (PEG) cloaking and molecular targeting. (B) A typical SEM image of PAA particles. (C) A typical size distribution result from multi-angle light scattering.

Source: Kopelman et al., 2005.

In-vitro test of Photofrin-containing nanoparticles for photodynamic therapy

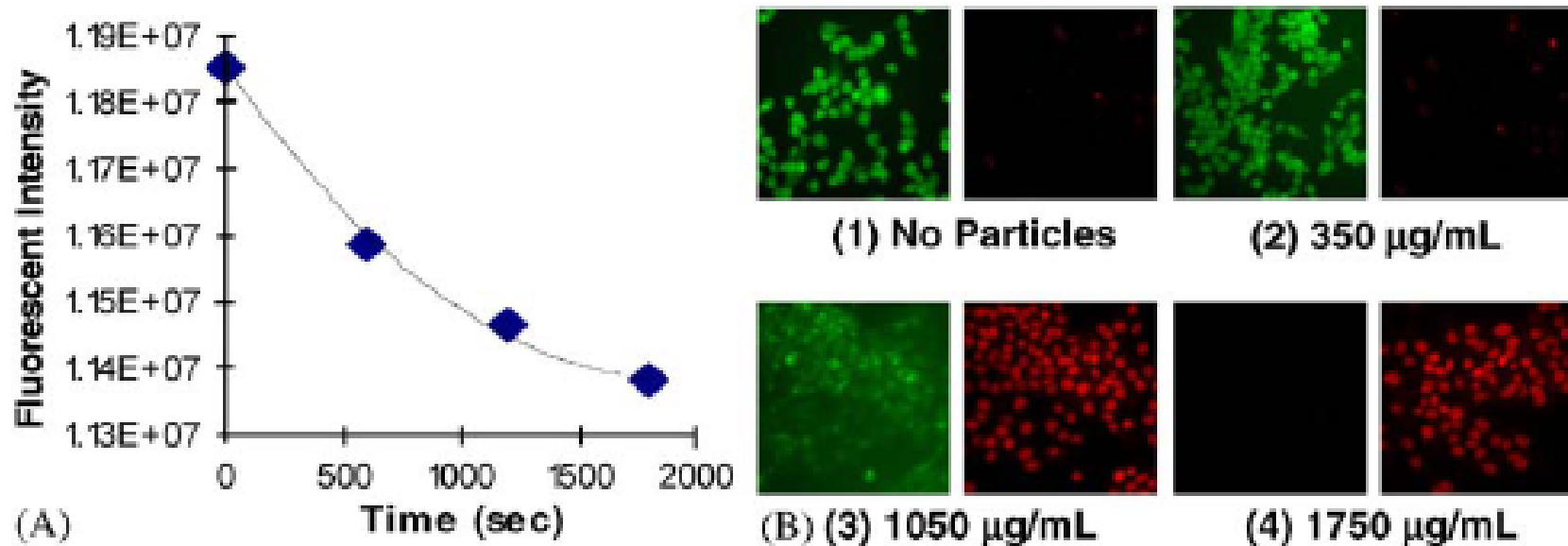


Fig. 2. (A) Detection of singlet oxygen produced by PHOTOFRINS-containing nanoparticles. The decay of fluorescence intensity of ADPA is a measure of singlet oxygen production and delivery by the nanoparticles. Excitation wavelengths: PHOTOFRINS (630 nm) and of ADPA (376 nm). (B) In vitro cell kill tests: dose response of PHOTOFRINS nanoparticles on cultured 9L cells: (1) no nanoparticles present; (2) 350 mg/mL nanoparticles present; (3) 1050 mg/mL nanoparticles present; (4) 1750 mg/mL nanoparticles present. The cells were exposed to 1500mW of 630nm laser light for 5 min. Calcein acetoxymethylester and propidium iodide were used to stain live and dead cells, respectively. For each pair of images, left-hand-side images show the live cells (green dots) while righthand-side images show the dead cells (red dots).

Source: Kopelman et al., 2005.

In-vivo MRI of nanoparticles containing Photofrin

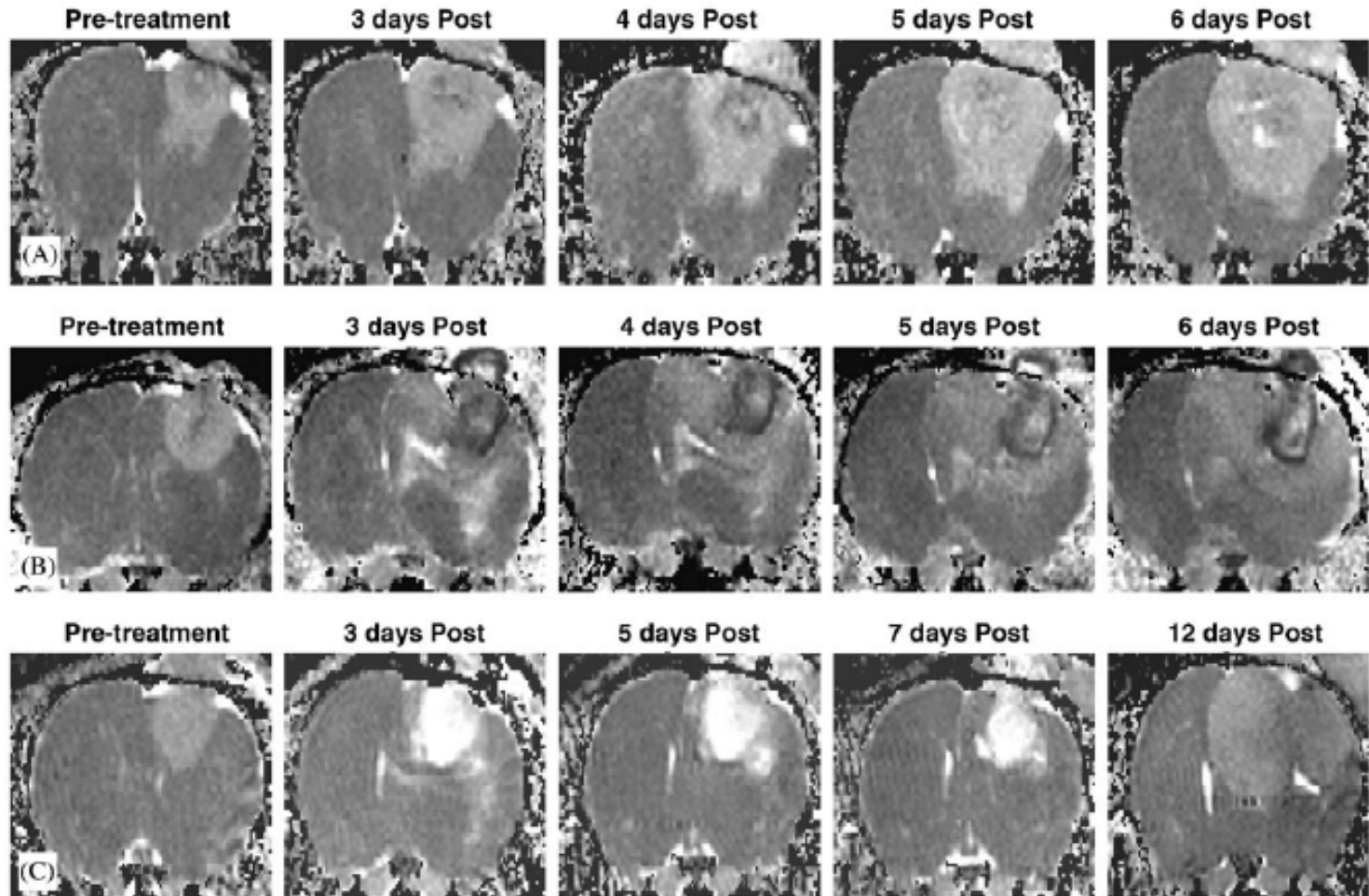


Fig. 3. Time series of the diffusion-weighted MR images of tumor after in vivo PDT: (A) untreated; (B) treated with laser light alone; (C) treated with laser light and PHOTOFRINS-containing PAA nanoparticles. The images shown here are not diffusion-weighted images but rather computer-generated quantitative diffusion maps wherein the intensity of each pixel (voxel) is proportional to the diffusion values for that voxel. Each series of images is obtained from a representative animal from a group of three.

Source: Kopelman et al., 2005.

In-vitro peptide (RGD) guided targeting of nanoparticles to cells

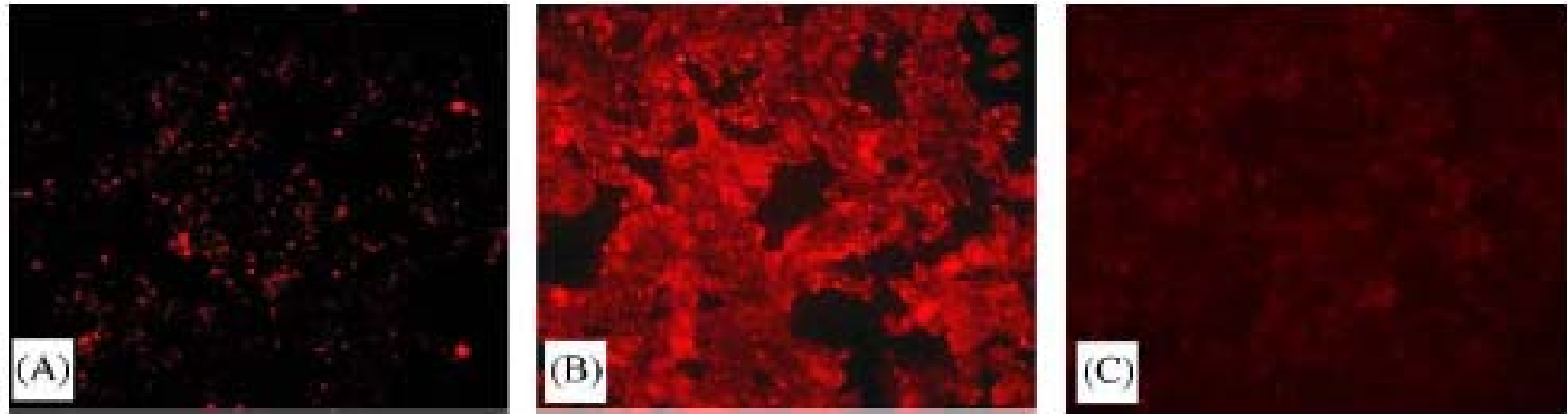


Fig. 5. RGD targeting of fluorescent nanoparticles to cell surface receptors on viable tumor cells. MDA-435 cells were used as a positive control and MCF-7 cells as a negative control. (A) Non-specific binding of non-targeted PAA-nanoparticles to MDA 435 cells. (B) RGD-modified nanoparticles selectively bind to MDA-435 cells. (C) RGD-modified nanoparticles do not bind MCF-7 cells.

Source: Kopelman et al., 2005.

IV. Examples of the in-vitro to in-vivo experimental pathway

Langer group – aptamer-targeted NPs for cancer therapy in-vivo

Source: Farokhzad, O.C., Cheng, J., Teply, B.J., Sherifi, I., Jon, S., Kantoff, P.W., Richie, J.P., Langer, R. Targeted nanoparticle-aptamer bioconjugates for cancer chemotherapy in vivo. PNAS 103(16), 6315–6320, 2006

Development of a nano- drug delivery system

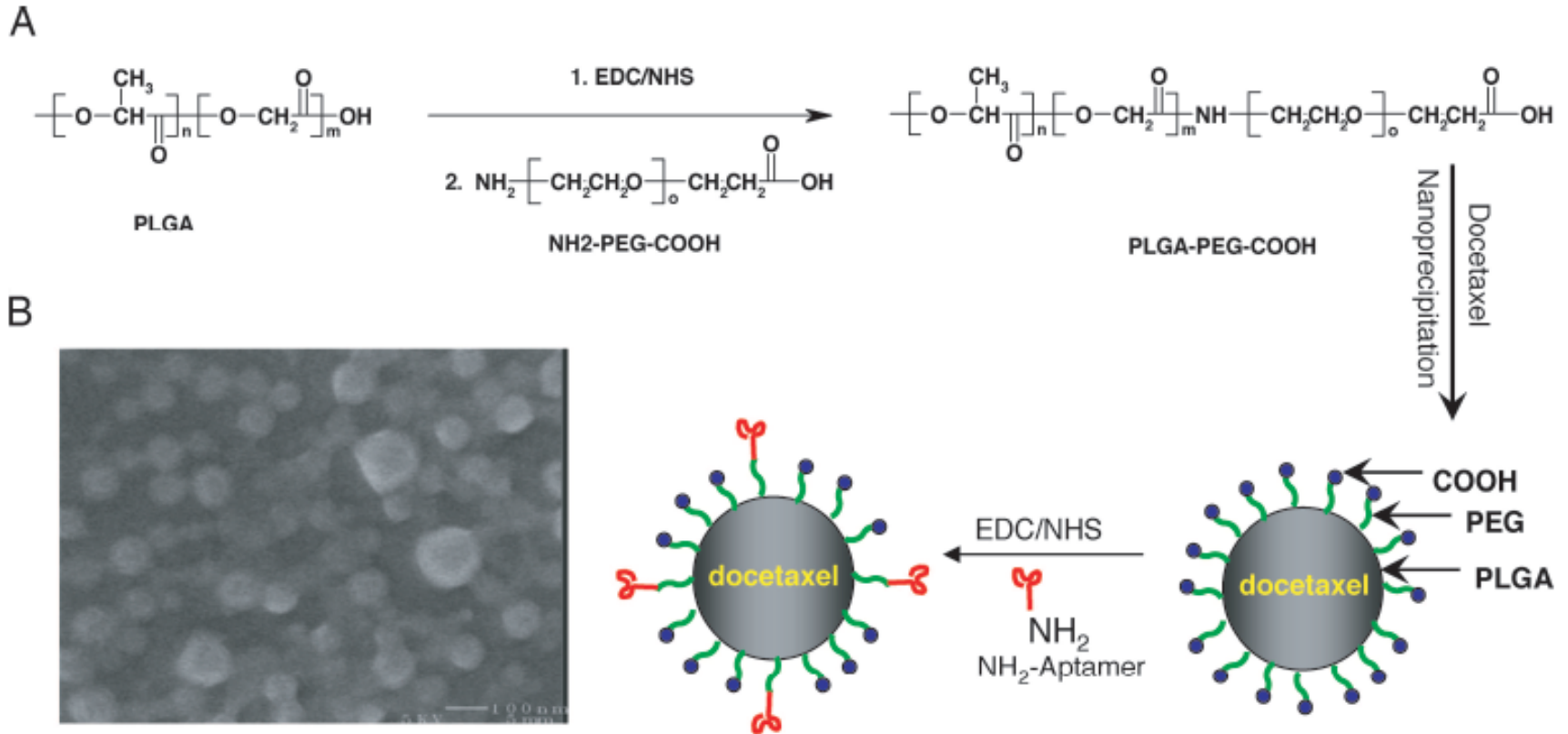


Fig. 1. Development of Dtxl-encapsulated pegylated PLGA NP-Apt bioconjugates. (A) Schematic representation of the synthesis of PLGA-PEG-COOH copolymer and strategy of encapsulation of Dtxl. We developed Dtxl-encapsulated, pegylated NPs by the nanoprecipitation method. These particles have a negative surface charge attributable to the carboxylic acid on the terminal end of the PEG. The NPs were conjugated to amine-functionalized A10 PSMA Apt by carbodiimide coupling chemistry. (B) Representative scanning electron microscopy image of resulting Dtxl-encapsulated NPs is shown. EDC, 1-ethyl-3-(3-dimethylaminopropyl)-carbodiimide; NHS, N-hydroxysuccinimide.

Efficacy studies of nano-drug delivery to human prostate cancer cells in nude mice

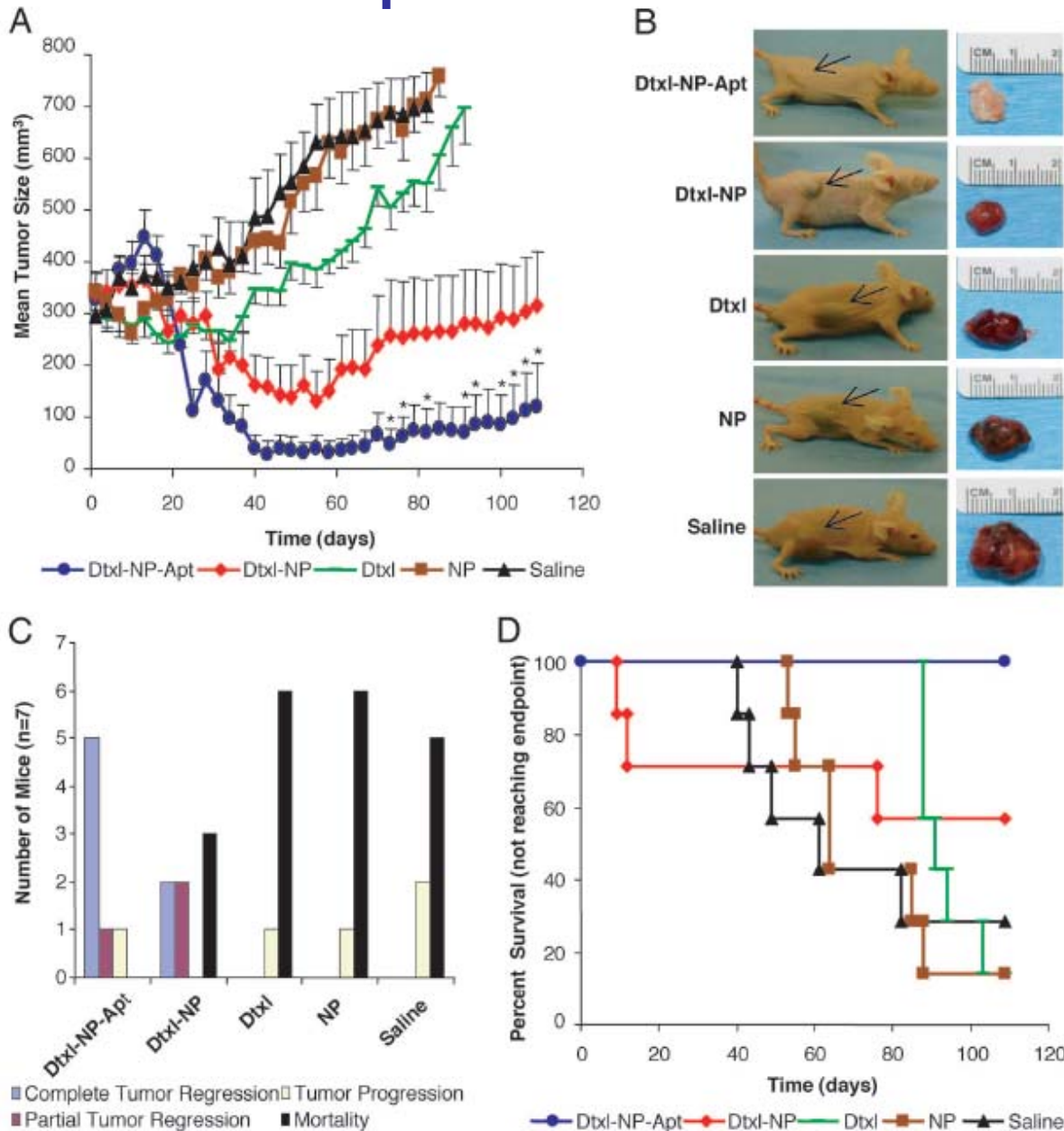


Fig. 3. Comparative efficacy study in LNCaP s.c. xenograft nude mouse model of PCa. (A) PCA was induced in mice by implanting LNCaP prostate epithelial cells s.c. in the flanks of nude mice and allowing the tumors to develop to appreciable size over 21 days (300 mm³). The comparative efficacy study of single intratumoral injection (day 0) of (i) saline (black); (ii) pegylated PLGA NP without drug (NP, brown); (iii) emulsified Dtxl (Dtxl, green), 40 mg/kg; (iv) Dtxl-ncapsulated NPs (Dtxl-NP, red), 40 mg/kg; or (v) Dtxl-encapsulated NP-Apt bioconjugates (Dtxl-NP-Apt, blue), 40 mg/kg was evaluated over 109 days and demonstrated that targeted NPs are significantly more efficacious in tumor reduction as compared with other groups. Data represent mean \pm SEM of seven mice per group. *, Data points for the Dtxl-NP-Apt group that were statistically significant compared with all other groups by ANOVA at 95% confidence interval. (B) Representative mouse at end point for each group is shown (Left) alongside images of excised tumors (Right). For the Dtxl-NP-Apt group, which achieved complete tumor regression, the scar tissue and underlying skin at the site of injection are shown. Black arrows point to the position of the implanted tumor on each mouse. (C) Plot of outcomes for each of the treatment groups divided into four categories: complete tumor regression (blue), incomplete tumor regression (red), tumor growth (yellow), and mortality (black). Two Dtxl-NP animals experienced >20% weight loss on days 9 and 12 after dosing and were euthanized. One mouse in each of the Dtxl and saline groups was euthanized late in the study for excessive weight loss likely attributable to large tumor load. (D) The Kaplan-Meier survival curve demonstrates that 100% of the Dtxl-NP-Apt group was alive on day 109, whereas the other groups had animals reaching our study end points and were euthanized on various days throughout the study period (end points defined as tumor load of 800 mm³ or BWL >20%).

Source: Farokhzad et al., 2006
12

Histological staining of the excised tumors

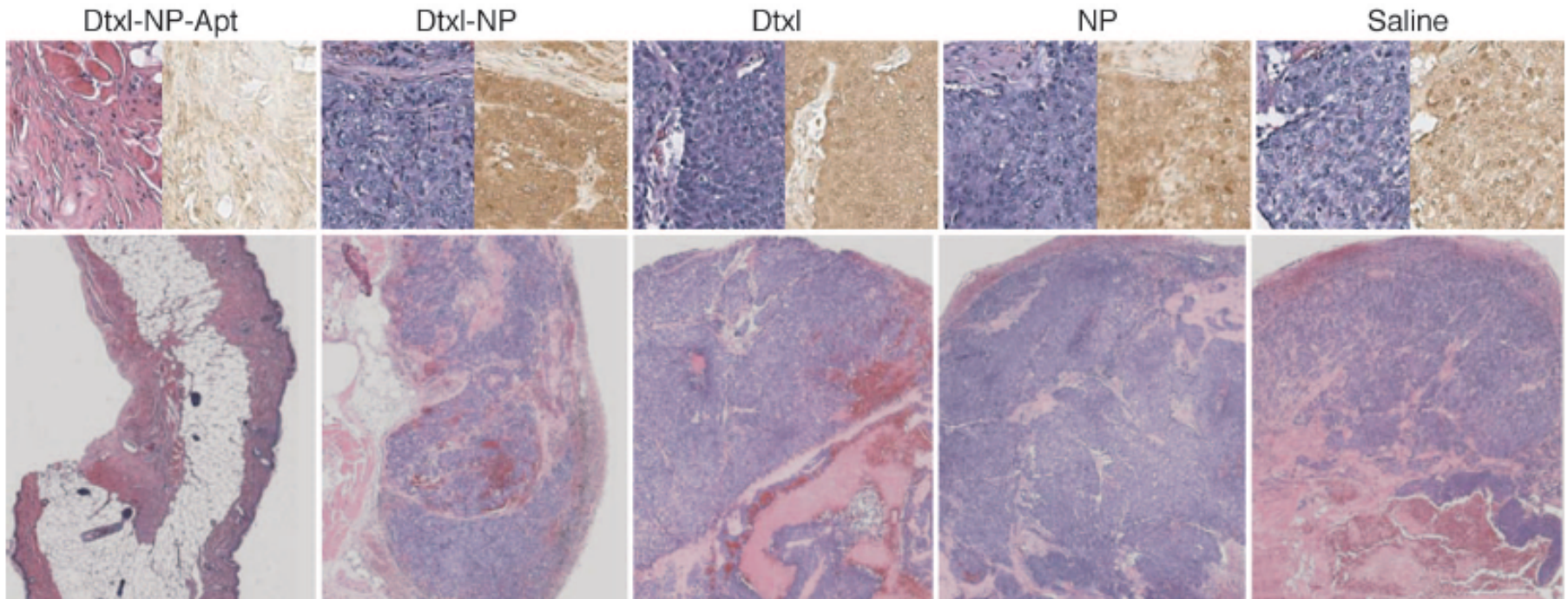


Fig. 4. Histological staining of the excised tumors in the (i) saline, (ii) pegylated PLGA NP without drug (NP), (iii) emulsified Dtxl (Dtxl), (iv) Dtxl-encapsulated NPs (Dtxl-NP), or (v) Dtxl-encapsulated NP-Apt bioconjugates (Dtxl-NP-Apt) was evaluated by an independent pathologist. The larger images (Lower) are H&E staining of representative specimens at $\times 20$ magnification. The smaller images (Upper) are H&E (Left) and PSMA (Right) staining of consecutive sections for each group at $\times 50$ magnification. All specimens except those obtained from the Dtxl-NP-Apt-treated mice were positive for PSMA staining [dark brown horseradish peroxidase stain]. The Dtxl-NP-Apt staining confirmed the absence of residual tumor and presence of scar and adipose tissue.

Source: Farokhzad et al., 2006

IV. Examples of the in-vitro to in-vivo experimental pathway

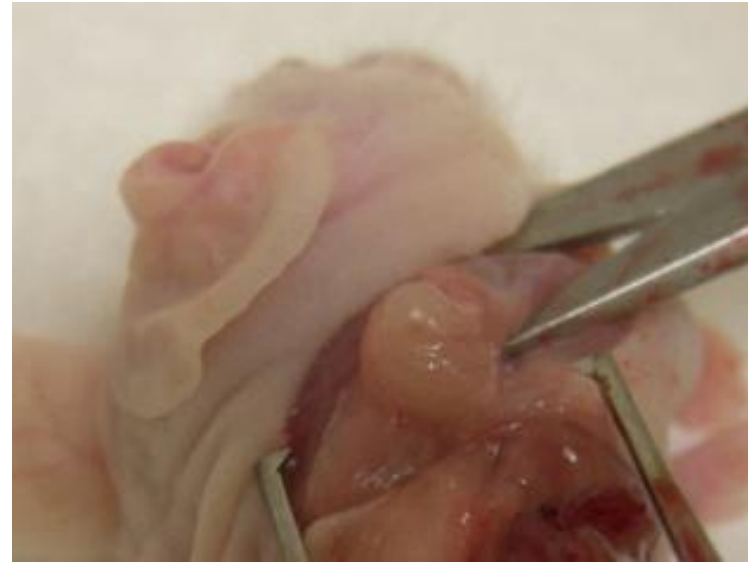
Leary group – work in progress:

- peptide-guided NPs to human tumors in nude mice
- magnetic nanoparticles as MRI contrast agents in tissue phantoms

Leary, J.F. "Design of Programmable, Multifunctional, Nanomedical Systems for Cancer Diagnostics and Therapeutics" presented at the FIFTH INTERNATIONAL NANOMEDICINE AND DRUG DELIVERY SYMPOSIUM, November 2–3, 2007, Northeastern University, Boston, MA.

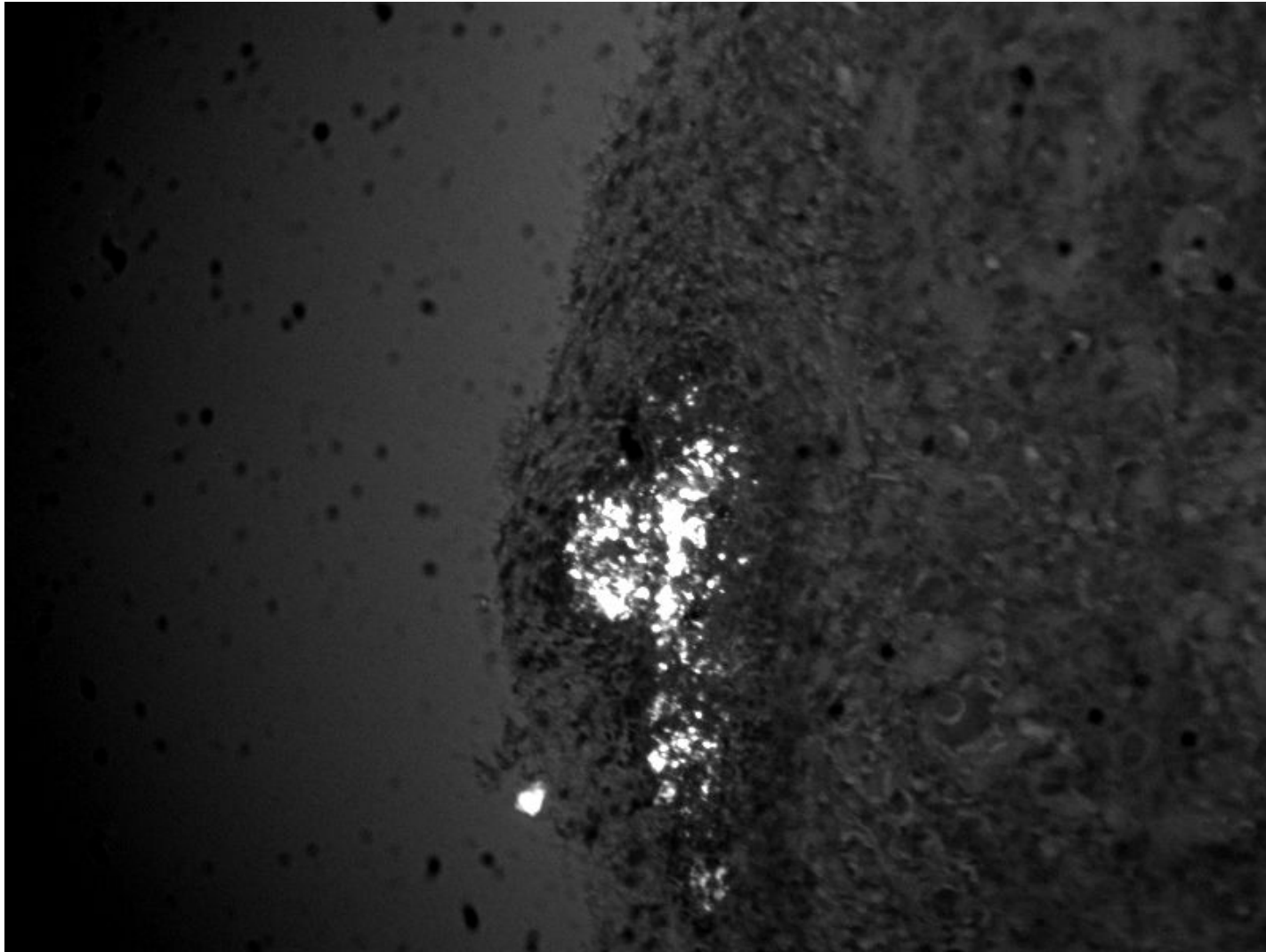
Some –in-vivo biodistribution studies

In-vivo peptide targeting of Qdot nanoparticles to human SKBr3 breast cancer cells in nude mice



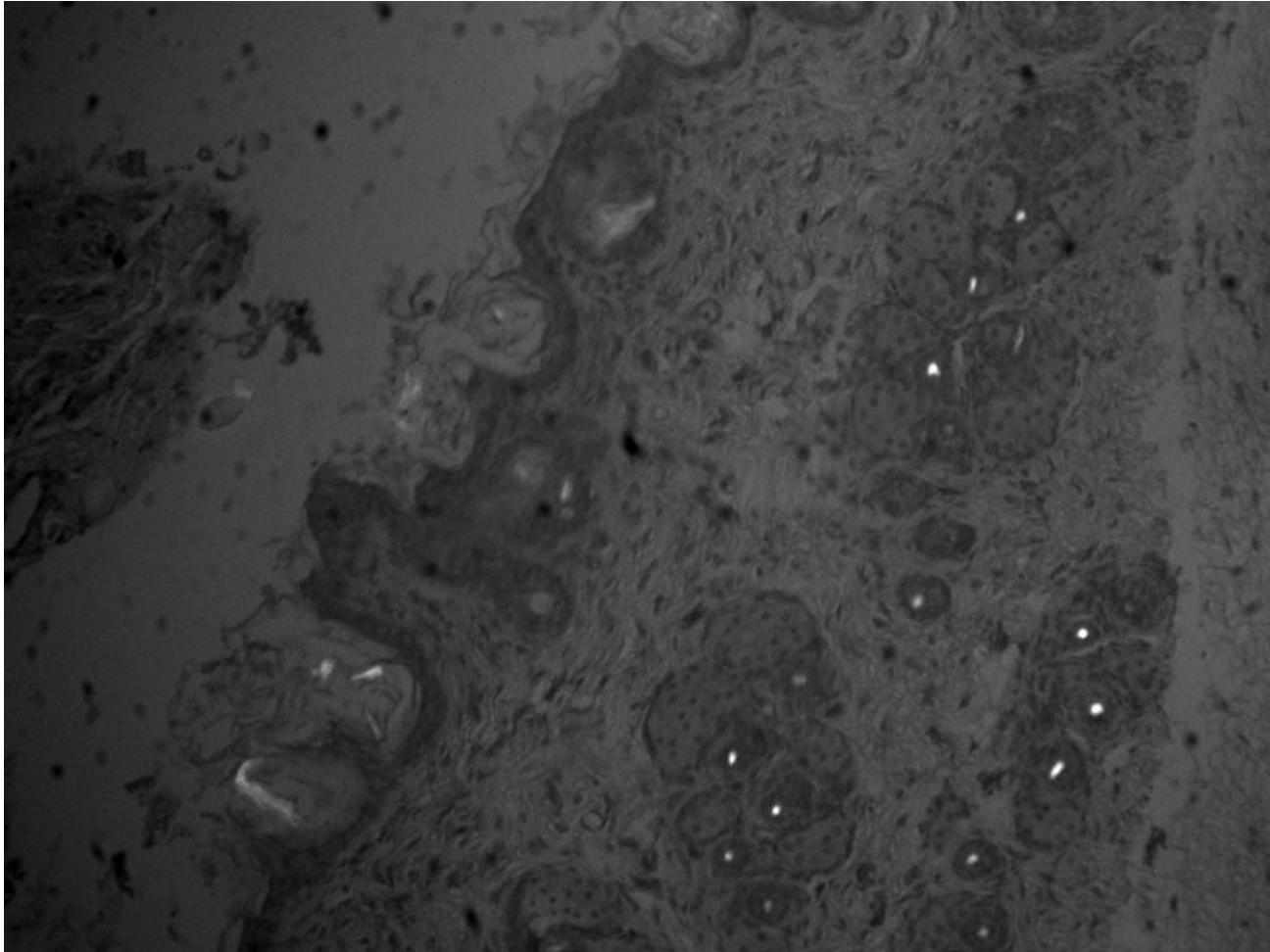
In collaboration with Dr. Deborah Knapp,
School of Veterinary Medicine, Purdue University
as part of the Masters thesis work of Emily Haglund

Qdots within SKBr3 human cell tumor grown in nude mice



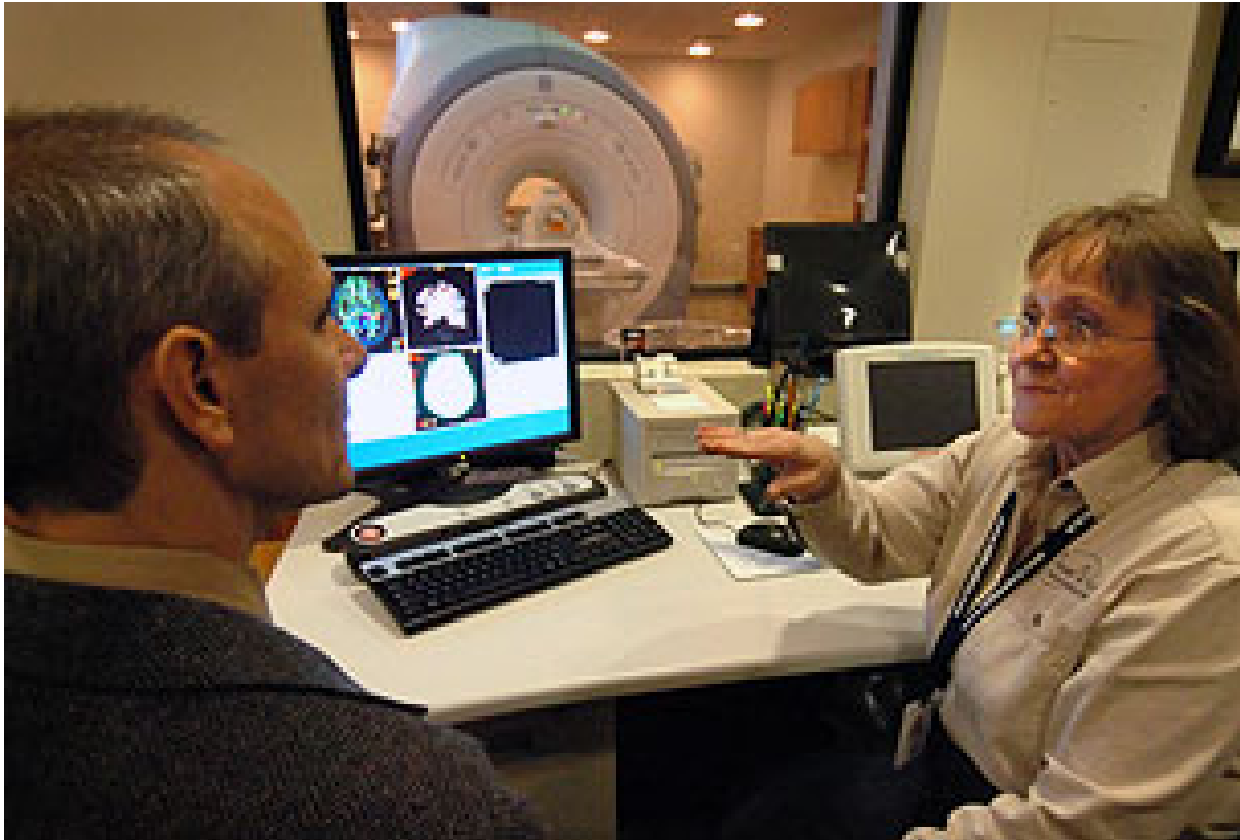
Positive control – Amino functionalized Qdots injected directly into subcutaneous tumor of nude mouse after its formation and vascularization.

SKBr3 human breast cancer cells targeted with peptide-guided Qdots



Peptide guided Qdots were injected into the tail veins of nude mice and processed into thin labeled histology sections (hematoxylin only, not eosin!) and imaged with a Q-Imaging, Inc. intensified camera on an inverted Nikon microscope.

New Purdue MRI 3-Tesla MRI now available for research use



updated: 11/2/2007 4:30:27 PM InsideIndianaBusiness.com Report

New Building Dedicated at Purdue Research Park

A new 26,000-square-foot building was dedicated Friday in the Purdue Research Park. The LakeView Technology Center will house a 7,800-square-foot MRI center called InnerVision West, which will include a high-powered MRI scanner. The building will also include space for Simulex Inc., a Purdue Research Park-based firm.

MRI Detection of Magnetic Nanoparticles in Tissue Phantoms

- Collagen gels were created to mimic *in vivo* tissue in order to create tumor-like mass of cells.
- Fluorescent staining of human breast cancer cells with Hoechst 33342 showed tumor-like formation within collagen gel
- Cancer cells were labeled magnetic nanoparticles (30nm iron oxide, OceanNanotech) using Lipofectamine 2000 (Invitrogen) to enhance MRI contrast

In collaboration with Drs. Thomas Talavadge and Charles Bouman, Weldon School of Biomedical Engineering, Purdue University

As part of the PHD thesis work of Mary-Margaret Seale

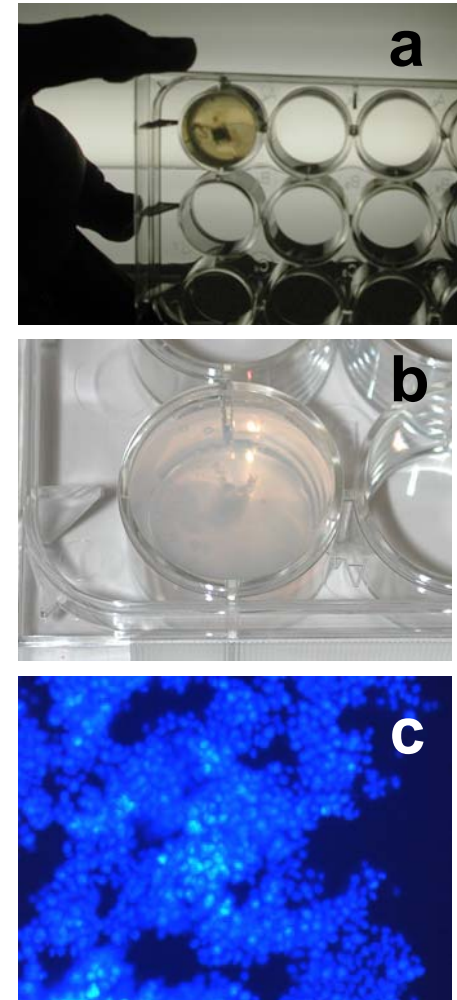
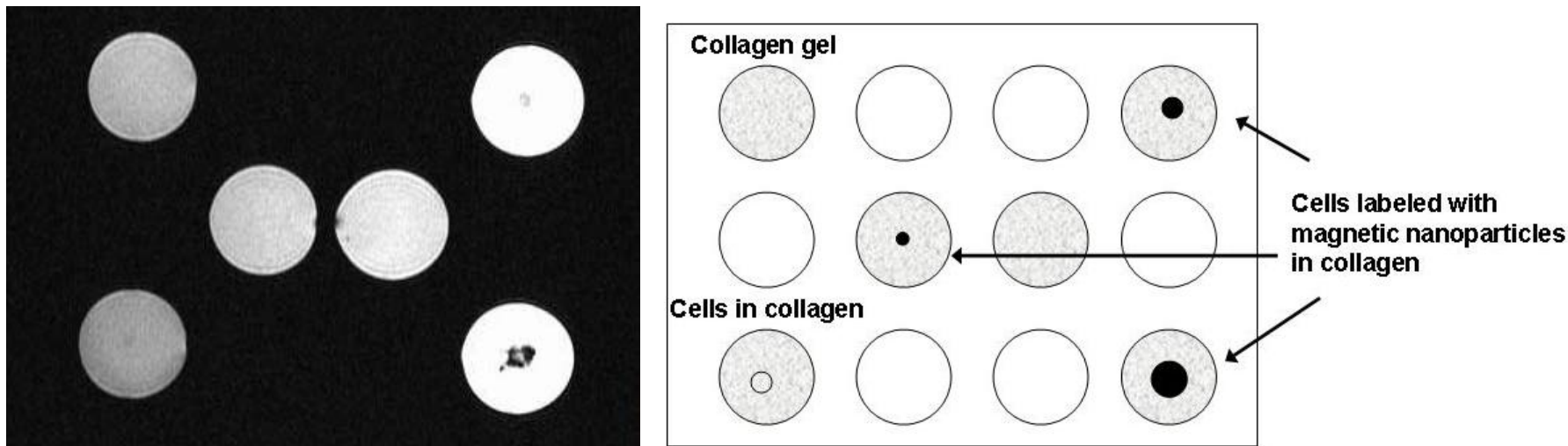


Figure 1. (a,b) Digital image of tumor like formation in 5mL collagen gel, (c) MDA-MB-231 human breast cancer cells stained with Hoechst 33342 in collagen gel.

MRI Detection of Magnetic Nanoparticles in Tissue Phantoms

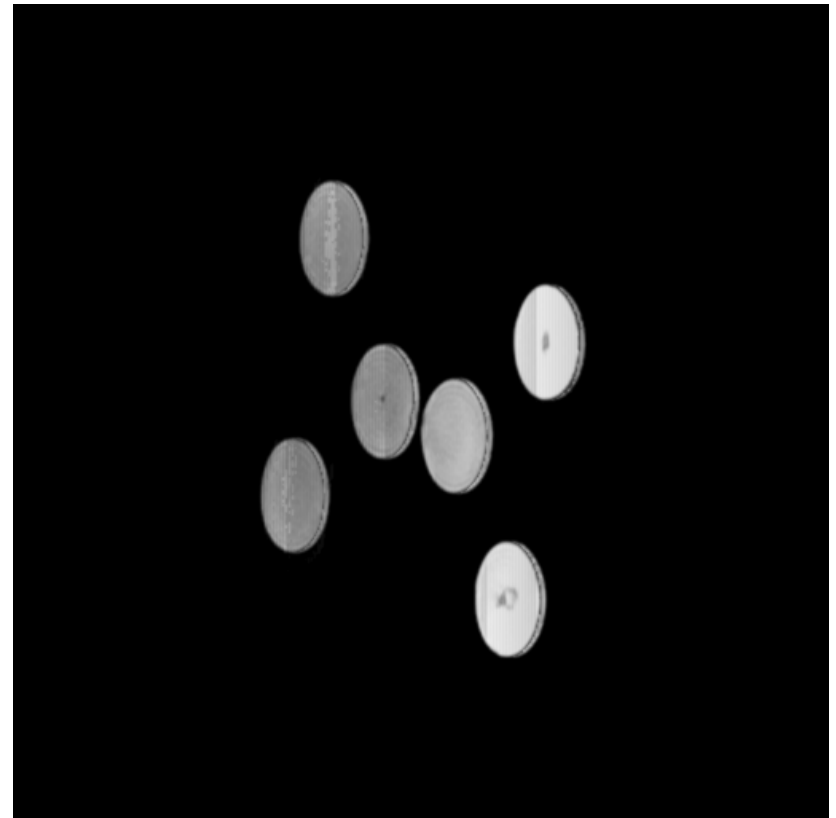
- Experimental setup for MRI scan: 12-well tissue culture plate



- Purpose is to determine MRI sensitivity to different sizes of 'tumors' labeled with magnetic nanoparticles
 - Tumor volumes approximately 400 μ L, 65 μ L and 5 μ L

MRI Detection of Magnetic Nanoparticles in Tissue Phantoms

- Coronal slices of T2-weighted fast spin echo show high contrast in labeled 'tumor' samples, especially compared to unlabeled cells
- Future experiments will focus on detection threshold cell number and nanoparticle concentration and material needed for in-vivo animal tests



References

Kopelman, R., Koo, Y-E, Philbert, M., Moffatc, B.A., Reddy, G.R., McConville, P., Hall, D.E., Chenevert, T.L., Bhojanie, M.S., Buck, S.M., Rehemtulla, A., Ross, B.D. Multifunctional nanoparticle platforms for in vivo MRI enhancement and photodynamic therapy of a rat brain cancer. *Journal of Magnetism and Magnetic Materials* 293: 404–410, 2005.

Farokhzad, O.C., Cheng, J., Teply, B.J., Sherifi, I., Jon, S., Kantoff, P.W., Richie, J.P., Langer, R. Targeted nanoparticle-aptamer bioconjugates for cancer chemotherapy in vivo. *PNAS* 103(16), 6315–6320, 2006